

Highlighting diffuse regions associated with young clusters: NGC 3590 beyond the stars

T. A. Sabino¹ & J. Gregorio-Hetem¹, S. Scarano Jr²

¹ Instituto de Astronomia, Geofísica e Ciências Atmosféricas, USP e-mail: thay.astro@gmail.com

² Departamento de Física, UFS

Abstract. Young stellar clusters are associated with star forming regions and play an important role in the chemical enrichment of our Galaxy. They are fundamental keys to understanding the formation and evolution of structures at galactic scales. Nonetheless, the processes related to the formation of clusters and the conditions of the medium in which they evolve are still open questions to be solved. Aiming to contribute to the current scenario, we conducted a detailed study of the gas conditions around the young stellar cluster NGC 3590 and the effects of stellar feedback based on SOAR/SAMI imaging observations in 4 bands with additional photometric data from 2MASS and AllWISE catalogs. We identified 37 members and 32 candidates, and 17 massive stars being part of the group. The comparative maps show the presence of diffuse regions that seem to delineate the cluster's structure of the core and its borders. It is remarkable the presence of a peculiar ring-like region surrounding 3 B-type stars, located northwest from the cluster's center. Beyond the medium around the massive stars, we also highlight the presence of a gradient in the H 1803 cloud's direction.

Resumo. Aglomerados estelares jovens são associados a regiões de formação estelar e desempenham um papel importante no enriquecimento químico da nossa Galáxia. Eles são peças fundamentais no entendimento da formação e evolução de estruturas em escalas galáticas. Além disso, os processos relacionados à formação dos aglomerados e as condições do meio em que eles evoluem permanecem como questões em aberto a serem resolvidas. Visando contribuir com o atual cenário, nós realizamos um estudo detalhado das condições do gás em torno do aglomerado estelar jovem NGC 3590 e efeitos de *feedback* estelar com base em imageamentos SOAR/SAMI em 4 bandas com dados fotométricos adicionais dos catálogos 2MASS e AllWISE. Nós identificamos 37 membros e 32 candidatas, assim como a presença de 17 estrelas massivas sendo parte do grupo. Os mapas comparativos mostram a presença de regiões difusas que parecem delinear a estrutura do núcleo do aglomerado e suas bordas. A presença de uma estrutura peculiar em forma de anel envolvendo 3 estrelas do tipo B é notável, localizada à noroeste do centro do aglomerado. Além do meio em torno das estrelas massivas, também destacamos a presença de um gradiente na direção da nuvem H 1803.

Keywords. Stars: formation – ISM: general – open clusters and associations: general

1. Introduction

Star forming regions are fundamental keys to understanding the formation and evolution of the Galactic structures and the present-day multi-band data acquisition techniques have improved the study of Young Stellar Clusters. Stellar parameters estimated through alternative methods have been established to evaluate physical features of the interstellar medium through the comparison between the light emission in distinct spectral ranges. Beyond that, the SOAR Telescope has shown to be a powerful tool in recent discoveries related to interstellar medium.

For instance, a detailed study of the Crab Nebula's morphology comparing NIR and visible light emission is presented by Loh et al.(2010; 2011) through SOAR/Spartan and HST narrow-band imaging in H₂, Br_γ, [S II] and [O III] bands, and has shown to be useful to delineate the smoothest structures within the Nebula. Moreover, Navarete et al.(2014; 2015) utilize SOAR/Spartan observations to evaluate the H₂ emission morphology around ~100 MYSOs and conclude that a large portion of the sample showed up in jet-like structures supporting the scenario in which massive stars are formed by accretion discs. More recently, Riaz et al.(2017) reported the discovery of the HH 1165, a new Herbig–Haro jet driven by a Proto-Brown Dwarf through SOAR narrow-band imaging in the H α , [S II] and R bands.

Aiming to contribute to the current scenario, we performed a detailed study of the gas conditions around NGC 3590 as well the effects produced by its own stars.

2. Methodology

In this work we use SOAR/SAMI 4-band imaging (R, H α , [S II] and [O III]) acquired during the observational run ID 20170221, complemented with the data from the catalogues Gaia EDR3/DR3 and 2MASS.

We use StarFinder to identify punctual sources positions and extract the background images from each of the exposures. We performed the astrometrical calibrations through Aladin, superposing Gaia EDR3 positions and DSS images to our fields. Using TopCat we correlated the previously identified sources in our fields to Gaia DR3 data to establish the membership criteria and determine clusters' members. We fitted Gaussian curves in the distributions of parallax and proper motions in right ascension and declination. The sources within 3σ in parallax and within 1σ and 3σ in proper motion were selected as members and candidates, respectively. We estimated ages through CMDs in Gaia DR3 G, G_{BP} and G_{RP} bands. Reddening corrections were made following Cardelli et al.(1989) and O'Donnell et al.(1994) A_V/A_V relations. The colour maps were generated through python scripts. The division of each of the exposures in distinct bands is the adopted technique to highlight structures in the field.

3. Results

Aiming to detect the main nebular structures in NGC 3590, our SAMI observations are centered at RA= $11^h12^m56^s$, Dec= $-60^\circ47'$ (J2000), that is, a $30''$ offset (northwest) from the clusters' center. So that our images show a stars' distribution misplaced from the center of the images. Thus, Figures 1-3 show that members and candidates are clustered around RA= $11^h13^m00^s$, Dec= $-60^\circ47'29''$ (J2000). Adopting as reference point the center of members distribution it is possible to highlight the following parts:

- The condensed central structure;
- The southern region;
- The northwest ring;
- The North and West zones where nebular emission is absent.

On the central region, which can be seen in purple shades on the $[S II]/[O III]$ map (see Fig. 2), are located not only the brightest - and massive - stars of the field but also it is the highest density region.

The southern region (Dec $< -60^\circ47'45''$), shown in reddish shades in all the colour maps, matches the H1803 dark cloud borders.

It is noticeable the presence of a structure around RA= $11^h12^m51^s$, Dec= $-60^\circ46'30''$ in a ring-like shape more evident on the $[S II]/[O III]$ map (see Fig. 2), indicating a weak $[S II]$ emission.

Outside the cluster's borders it is noted the presence of a region shown in purple and bluish shades on the $H\alpha/[S II]$ and $H\alpha/[O III]$ maps (see Figs. 1 and 3). Even though those regions are rich in stars, just a few of them were selected as members of our cluster. Furthermore, there is no evidence of nebular emission on those areas in other wavelengths.

In Figure 1, the gradient in the southern region of NGC 3590 and the central column ($H\alpha/[S II] > 3$) are remarkable and indicate the presence of excited gas, following the distribution of the diffuse emission also seen in the infrared. The higher $H\alpha$ emission delineates the distribution of low-velocity shocks.

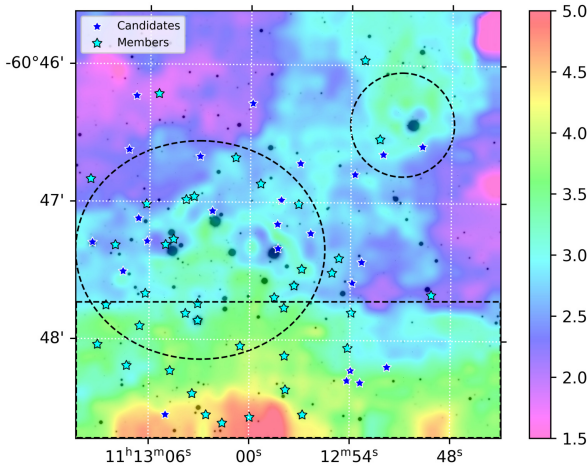


FIGURE 1. Map resulting from the images ratio $H\alpha/[S II]$ for NGC 3590.

The northwest ring-like structure shows up as a nebular structure extended up to the south, in which the $H\alpha/[S II]$ ratio reaches values higher than 5, coinciding with the direction of the H 1803 cloud.

In Figure 2, the large regions shown in purple shades ($[S II]/[O III] < 0.35$) in the cluster's core and in the northern annulus highlight the presence of ionized gas. The higher ratio shows that the major part of the low-ionization gas is located outside the cluster's border and away from the brightest stars. The lower values ($[S II]/[O III] < 0.35$) in the central region of NGC 3590 match with the massive stars location and may be associated with absence of gas in that region due to the stars feedback effects on the environment.

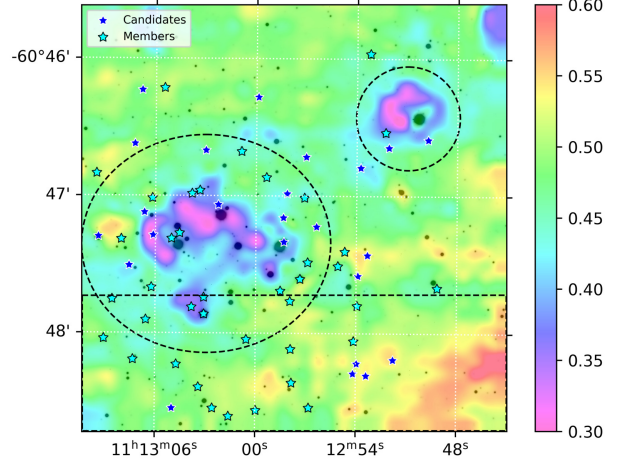


FIGURE 2. Map resulting from the images ratio $[S II]/[O III]$ for NGC 3590.

The $H\alpha/[O III]$ map (Fig. 3) shows that the higher ratio (> 1.25) delineates the major structures extended from the northwest to the south, till the H1803 Cloud border, in which the ratio is superior to 2.25. On the environment around the massive stars, the $H\alpha/[O III]$ ratio falls under 0.75.

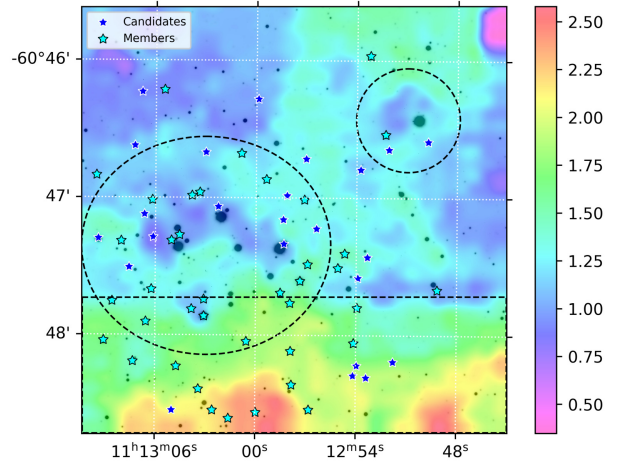


FIGURE 3. Map resulting from the images ratio $H\alpha/[O III]$ for NGC 3590.

3.1. Detailed view on the central region of NGC 3590

The central region of NGC 3590 is defined by the $1.8' \times 1.8'$ section centered at RA= $11^h13^m02^s$, Dec= $-60^\circ47'19''$ (J2000),

which contains the largest density of stars on the field. This region was previously described by Piatti et al.(2010) as the delimitation of NGC 3590 and, lately, Molina-Lera et al.(2016) delineated the cluster's extension up to $4'$.

The massive stars are located on this region and it is notable the existence of some peculiar features not only around those massive stars but within the environment as a whole.

Intermediate values of $H\alpha/[S II]$ ratio in this region seem to surround the brightest stars of the group, producing the greenish and yellow patterns ($3 < H\alpha/[S II] < 3.75$) shown on the center of the map in the Figure 4. Those structures may be associated with shock fronts due to the massive stars feedback effects. Beyond that, the gradient in the H 1803 cloud's direction is also significant, in which the $H\alpha/[S II]$ ratio reaches over 3.75 in the southern limits of the map, while in the peripheral zone of the cluster (shown in purple shades) the ratio fall under 2.25.

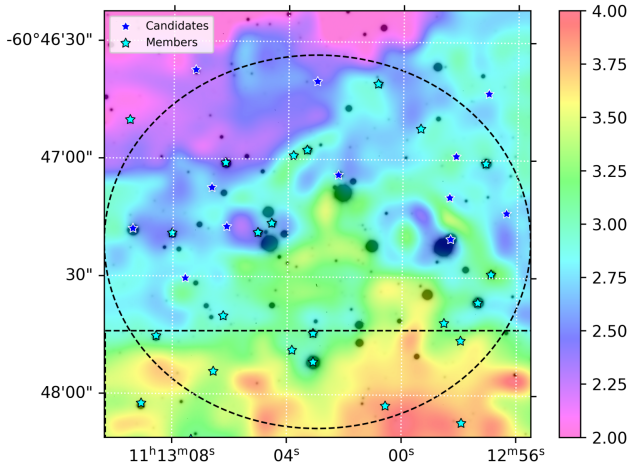


FIGURE 4. Map resulting from the images ratio $H\alpha/[S II]$ for NGC 3590.

The $[S II]/[O III]$ map (Fig. 5) reveals a region in which there is a higher concentration of low-ionization gas ($[S II]/[O III] > 0.45$), shown in greenish shades, and the medium around the massive stars ($[S II]/[O III] < 0.35$), shown in purple shades.

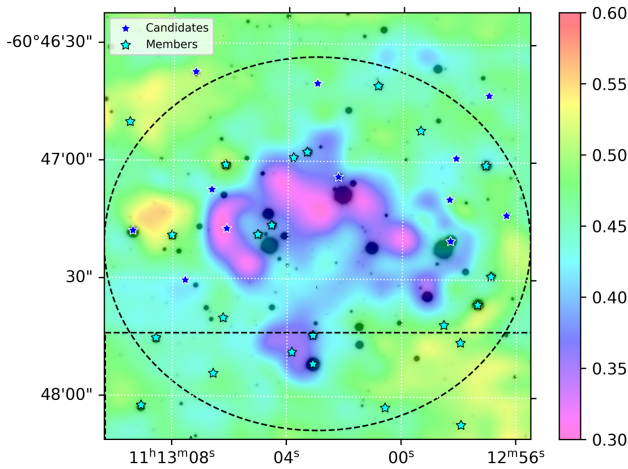


FIGURE 5. Map resulting from the images ratio $[S II]/[O III]$ for NGC 3590.

Evidences of neutral and ionised gas over-densities on the field can be traced by the $H\alpha/[O III]$ indicator (see Fig. 6). The higher fraction on the south ($H\alpha/[O III] > 1.8$) indicates a significant contribution of neutral gas emission in the H1803 cloud direction when compared to its vicinity, while the region surrounding the massive stars shows $H\alpha/[O III] < 1$, indicating ionised gas predominance in the region.

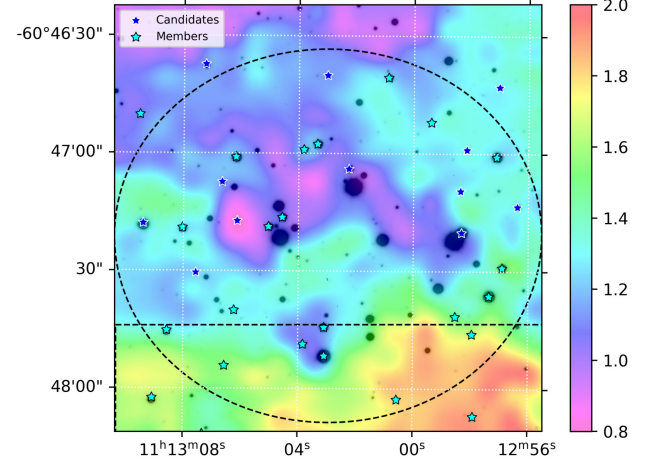


FIGURE 6. Map resulting from the images ratio $H\alpha/[O III]$ for NGC 3590.

4. Conclusion

Our results have shown that the interstellar medium of Young Stellar Clusters can be detected through SOAR/SAMI and we could identify the main features of the cluster. We identify 37 members, 32 candidates and 17 massive stars being part of the group. The comparative maps show the presence of diffuse regions that seem to delineate the cluster's structure of the core and its borders. It is remarkable the presence of a ring-like region surrounding 3 B-type stars. This peculiar structure is located northwest from the cluster's center, being the farthest - from the cluster's core - structure identified by us. Beyond the medium around the massive stars, we also highlight the presence of a gradient in the H 1803 cloud's direction.

Acknowledgements. We are thankful to FAPESP for the financial support (Proc. No. 2023/08726-2 and 2024/01288-2).

References

- Cardelli, J. A., Clayton, G. C., & Mathis, J. S. 1989, *ApJ*, 345, 245, doi: 10.1086/167900
- Loh, E. D., Baldwin, J. A., & Ferland, G. J. 2010, *ApJ*, 716, L9, doi: 10.1088/2041-8205/716/1/L9
- Loh, E. D., Baldwin, J. A., Curtis, Z. K., et al. 2011, *ApJS*, 194, 30, doi: 10.1088/0067-0049/194/2/30
- Molina-Lera, J. A., Baume, G., Gamen, R., Costa, E., & Carraro, G. 2016, *Astronomy and Astrophysics*, 592, A149, doi: 10.1051/0004-6361/201527926
- Navarete, F., Damineli, A., Barbosa, C. L., & Blum, R. D. 2014, in *Revista Mexicana de Astronomia y Astrofisica Conference Series*, Vol. 44, 142–142
- Navarete, F., Damineli, A., Barbosa, C. L., & Blum, R. D. 2015, *MNRAS*, 450, 4364, doi: 10.1093/mnras/stv914
- O'Donnell, J. E. 1994, *ApJ*, 422, 158, doi: 10.1086/173713
- Piatti, A. E., Clariá, J. J., & Ahumada, A. V. 2010, *PASP*, 122, 516, doi: 10.1086/652501
- Riaz, B., Briceño, C., Whelan, E. T., & Heathcote, S. 2017, *The Astrophysical Journal*, 844, 47, doi: 10.3847/1538-4357/aa70e8